MOLECULAR PHYSICS, 1990, VOL. 69, NO. 2, 265–280

Internal rotation in 1,4-dimethylnaphthalene studied by high resolution laser spectroscopy

by PAUL UIJT DE HAAG, RUDIE SPOOREN†, MAARTEN EBBEN and LEO MEERTS

Fysisch Laboratorium, Katholieke Universiteit, Toernooiveld, 6525 ED Nijmegen, The Netherlands

and JON T. HOUGEN‡

Molecular Spectroscopy Division, National Institute of Standards and Technolgy, Gaithersburg, Maryland 20899, U.S.A.

(*Received 11 July 1989; accepted 25 July 1989*)

The high resolution laser induced fluorescence spectrum of the 0_0^0 $S_1(^1A_1) \leftarrow S_0(^1A_1)$ electronic transition in 1,4-dimethylnaphthalene has been studied in a molecular beam. The residual Doppler width of 12 MHz allowed rotational resolution and the study of the effects of the internal rotation of the two methyl groups. All strong lines were assigned and the rotational constants in both the ground and excited electronic states were determined. The internal rotation of the two methyl groups manifests itself in the spectrum by a splitting of each rotational transition into three lines. The splitting of the lines is 40 ± 1 MHz and constant up to $J = 11$ and $K_{+1} = 11$. The intensity ratio of the lines is 1 : 2 : 1 within 10 per cent. No further splittings were observed in the investigated frequency range. It is shown that the spectrum is totally explained by the simple model of two independent internal rotors attached to an asymmetric rotor frame. The effect of the interaction of the two rotors is negligible with the present resolution as is the effect of the interaction between internal rotation and overall rotation. The measured splittting of 40 MHz yields information about the barriers to internal rotation in the two electronic states. With some assumptions a barrier height of $570 \pm 10\,\mathrm{cm}^{-1}$ in the excited S_1 state is deduced.

1. Introduction

Hindered internal rotation of a methyl group attached to an asymmetric rotor frame has been a subject of research for some time, and many different techniques have been used [1]. The best known determinations of barrier shapes and barrier heights stem from microwave spectroscopy. With this method one probes directly the splittings in the energy states due to the hindered rotation. There are however some severe limitations to this method. The molecules must possess a permanent electric dipole moment to exhibit a microwave spectrum, while for symmetric top molecules the selection rule $\Delta K = 0$ hampers the direct observation of the torsional splittings. Therefore symmetric top molecules are studied by other methods like the

† Present address: NTH, Institutt for Fysikk, Sem Saelandsvei 7, N-7034 Trondheim, Norway.

‡ Nederlandse organisatie voor Wetenschappelijk Onderzoek, visiting scientist University of Nijmegen, spring 1988.

0026–8976/90 $3.00

avoided crossing molecular beam technique [2]. However, for a large molecule the microwave spectrum is rather complex. This makes it difficult to unravel the effect of the internal rotation.

A different approach is the direct observation of the torsional vibrations either by infrared absorption spectroscopy or by Raman spectroscopy. Especially the overtones of the torsional vibration give information about the barrier heights and barrier shapes. These torsional vibrations can also be seen in the fluorescence excitation spectrum of an excited electronic state [3]. By measuring in the dispersed fluorescence spectrum progressions in the ground state torsional vibration information is obtained about the barrier to internal rotation in the electronic ground state. In the same way information about the barrier in the excited electronic state can be deduced from progressions of the torsional vibration in the fluorescence excitation spectrum. It is clear however that high barriers in a large molecule will produce torsional vibrations hardly distinguishable from the normal vibrations. On the other hand, a low barrier will produce spectral features undetectable at medium resolution.

These limitations can be overcome by the measurement of the fluorescence excitation spectrum of an excited electronic state with high resolution in a cold molecular beam. Like in microwave spectroscopy information on the barrier height to internal rotation is deduced from the splittings in the energy states. The strong rotational cooling in the molecular beam reduces the complexity of the electronic spectrum considerably. However, in this method two electronic states are involved and we probe the difference in splittings in the electronic states. As we will show , it is in principle still possible to determine from the high resolution spectrum the barrier heights to internal rotation in both electronic states independently.

We report here the high resolution fluorescence excitation spectrum of the 0_0^0 $S_1 \leftarrow S_0$ electronic transition in 1,4-dimethylnaphthalene (1,4-DMN) in a cold molecular beam. In these large molecules the interaction between the two methyl groups takes place via the conjugated electron system of the frame. Up to now little is known about the internal rotation and couplings in such molecules. The fluorescence excitation spectrum at medium resolution performed in a molecular jet is published elsewhere [4]. Previous data on the internal rotation in 1,4-DMN stem from nuclear spin relaxation measurements in the solid state phase [5]. The resulting barrier to internal rotation in the electronic ground state was found to be about 2.2 kcal/mole (770 cm^{-1}). This relatively high barrier allows us to use the high barrier approximation in the analysis of our results.

2. Experimental

The experimental set up is already described elsewhere [6]. Briefly, a molecular beam was formed by a continuous expansion of 1,4-DMN seeded in argon through a nozzle with a diameter of 75 μm. The sample of 1,4-DMN was heated to a temperature of 80°C in order to achieve enough vapour pressure. The backing pressure of argon was varied between 0·25–1·5 bar. In this way the rotational temperature of the ensemble of molecules in the molecular beam was varied. This facilitated the analysis of the spectrum considerably. To reduce the Doppler width, the molecular beam was strongly collimated by two conical skimmers with a diameter of 1·5 mm in a differential pumping system. The molecular beam was chopped at a rate of 16 Hz, allowing phase sensitive detection.

Excitation of the molecules took place 30 cm downstream from the nozzle by the continuous wave radiation field of an intracavity frequency doubled ring dye laser (a modified Spectra Physics 380D). By using an angle tuned $LiIO_3$ crystal, about 2 mW of single frequency U.V. radiation was obtained. The laser line width was about 3 MHz and stabilized scans of 120 GHz could be made. The total line width of a single line in the spectrum was 12 MHz and was dominated by the residual Doppler width in the molecular beam. For relative frequency measurements a part of the fundamental laser beam was sent to a sealed off, temperature stabilized Fabry–Perot interferometer. The line width of 12 MHz in the spectrum allowed relative frequency measurements with an accuracy of 3 MHz. However, frequency drift in the interferometer was the dominating source of errors when relative frequencies over 1 GHz were measured. For absolute frequency measurements the absorption spectrum of iodine was recorded simultaneously [7]. The accuracy in the absolute frequency measurement was determined by the line width in the recorded iodine absorption spectrum. This line width was about 850 MHz.

The total undispersed laser induced fluorescence was collected by two spherical mirrors and imaged on the photocathode of a photomultiplier (EMI 9789QA). The signals were processed by a standard photon counting system (Ortec Brookdeal 5C1) interfaced with a PDP 11/23+ computer. Further reduction of the spectra was also done on the computer.

3. Results and asymmetric rotor analysis

With the experimental set up described we have measured the $0_0^0 S_1 \leftarrow S_0$ transition in 1,4-DMN. A part of the spectrum is shown in figure 1. The spectrum is obtained with 1 mW of U.V. radiation and with 0·5 bar backing pressure of the seeding gas argon. The line width in the spectrum is 12 MHz. Due to the high density of spectral lines more than half of the lines in the spectrum were overlapping. The intensities were typically in the order of 5000 counts per second per mW U.V. radiation.

In a low density region of the spectrum it is easy to see that every rotational transition consists of a group of three lines. This is visible in the insert in figure 1. The splitting of these lines is 40 ± 1 MHz and constant at the precision of measurement throughout the whole investigated frequency range. Furthermore no additional splittings were observed in the investigated frequency range. The intensity ratio of the three lines is 1 : 2 : 1 within the accuracy in the measured intensities of 10 per cent. It seems clear that this splitting is due to the internal rotation of the two methyl groups. Because the splitting of 40 MHz is constant over the whole investigated frequency range we chose the central line of each group of three lines for a rotational analysis of the spectrum. The analysis of the rotational spectrum was facilitated by an estimated structure of the 1,4-DMN molecule and the results of earlier performed laser induced fluorescence measurements on the electronic transition in naphtalene [6]. The 1,4-DMN molecule is a near oblate symmetric top with the *a*-, *b*- and *c*-axis as indicated in figure 2. The results for naphthalene showed that the vibrationless electronic transition is polarized along the *a*-axis [6]. This axis corresponds to the *a*-axis in the 1,4-DMN molecule. We started with the assumption that the direction of the transition dipole moment is not changed by the addition of the two methyl groups.

About 200 lines in the central 30 GHz of the spectrum up to $J = 13$ were assigned. In the congested central region of the spectrum use was made of the

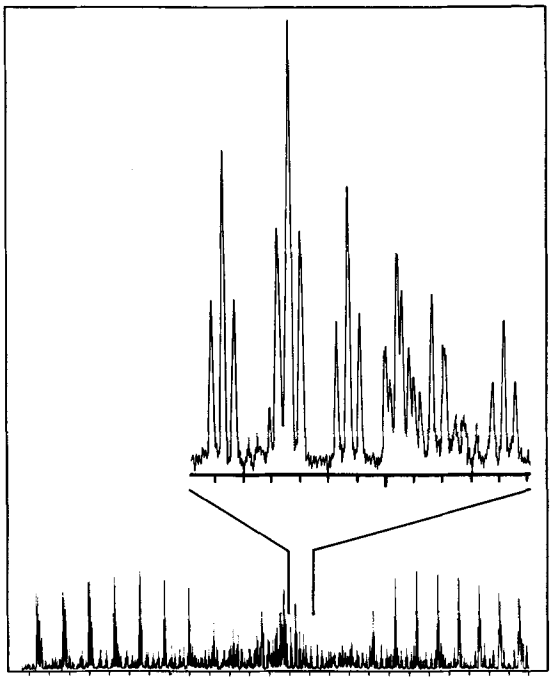

Figure 1. Part of the laser induced fluorescence spectrum of the 0_0^0 $S_1 \leftarrow S_0$ electronic transition in 1,4-DMN. The frequency is marked every GHz and increases from left to right. The insert gives an exploded view of the spectrum, showing clearly the groups of three lines. Here the frequency is marked every 100 MHz.

recordings with different backing pressures. In figure 3 parts of these spectra are shown. In this way it was possible to identify unambiguously the transitions where states with low quantum number J were involved. It turned out that it was possible to fit the observed transitions to an asymmetric rotor hamiltonian. The fit was made

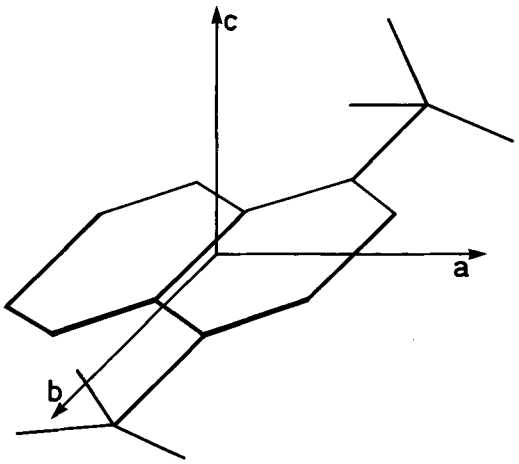

Figure 2. The 1,4-dimethylnaphthalene molecule with the principal axes of inertia *a*, *b* and *c*. The measured electronic transition is polarized along the *a*-axis.

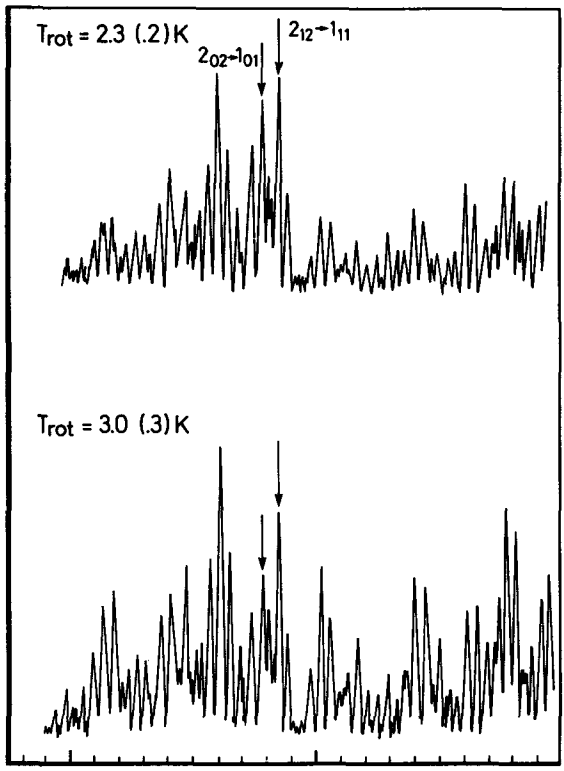

Figure 3. Part of the laser induced fluorescence spectra of the 0_0^0 $S_1 \leftarrow S_0$ electronic transition at two different rotational temperatures. The frequency is marked every 100 MHz and increases from left to right. Rotational transitions are indicated by $J''_{K_{-1}''K_{+1}''} \rightarrow J'_{K_{-1}'K_{+1}'}$.

to a perpendicular *a*-type transition, in accordance with the results for naphthalene. This established the symmetry of the excited S_1 state to be $^1A_1$ in the molecular point group C_{2v}. A least squares fit of the observed transitions to the asymmetric rotor hamiltonian yielded the effective rotational constants in both ground and excited electronic state. The standard deviation of the fit was 4·6 MHz, well within the experimental line width. Table 1 lists the frequencies of the transitions used in the asymmetric rotor fit with identification, and the obtained molecular constants are given in table 2. The indicated errors are determined by the fit. The dominant source of errors is however the drift of the interferometer. The magnitude of this error can be estimated by comparison of different scans and is about four times the error determined by the fit. The absolute frequency of the transition ν_0 was determined with the use of the iodine absorption spectrum. Here the indicated error is due to the accuracy in the measurement of the iodine absorption line positions.

The relative intensities of single rotational lines, assuming a Boltzmann distribution in the molecular beam, is given by

$$I = I_0(2J'' + 1)g_n A_{J''K_{-1}''K+1''} \exp\left[-E(J'', K''_{-1}, K''_{+1})/kT_{\text{rot}}\right] . \qquad (1)$$

In this equation J'', K''_{-1}, K''_{+1} are the rotational quantum numbers of the electronic ground state, g_n are the statistical weights due to the nuclear spin, $A_{J''K_{-1}''K_{+1}''}$ are the Hönl–London factors and $E(J'', K''_{-1}, K''_{+1})$ is the energy of the electronic

Table 1. Observed rotational transitions of the vibrationless $S_1 \leftarrow S_0$ electronic transition in 1,4-DMN. Frequencies are given relative to the origin at 31491·553 cm^{-1}.

Observed Frequency/MHz	Calculated Frequency/MHz	Obs.-calc. Frequency/MHz	Identification					
			J''	K''_{-1}	K''_{+1}	J'	K'_{-1}	K'_{+1}
−14218·2	−14209·0	−9·2	11	1	11	10	1	10
−14170·1	−14156·8	−13·3	10	2	9	9	2	8
−14083·7	−14074·4	−9·3	9	3	7	8	3	6
−13975·8	−13963·6	−12·2	8	4	5	7	4	4
−13696·3	−13685·7	−10·6	7	5	3	6	5	2
−12888·5	−12888·3	−0·2	10	1	10	9	1	9
−12839·0	−12836·4	−2·6	9	2	8	8	2	7
−12757·2	−12754·6	−2·6	8	3	6	7	3	5
−12659·7	−12663·8	4·1	7	3	4	6	3	3
−12659·7	−12655·2	−4·5	6	4	2	4	4	1
−12636·3	−12636·4	0·1	7	4	4	6	4	3
−12086·5	−12083·7	−2·8	11	2	9	11	2	10
−11990·9	−11986·3	−4·6	6	5	2	5	5	1
−11578·3	−11583·5	5·2	9	1	9	8	1	8
−11527·5	−11532·0	4·5	8	2	7	7	2	6
−11448·2	−11450·9	2·7	7	3	5	6	3	4
−11266·3	−11265·5	−0·8	6	4	3	5	4	2
−11097·9	−11093·4	−4·5	11	3	8	11	3	9
−10865·3	−10861·1	−4·2	13	6	7	13	6	8
−10748·3	−10749·1	0·8	10	2	8	10	2	9
−10442·8	−10435·6	−7·2	9	1	8	9	1	9
−10463·6	−10458·2	−5·4	12	5	7	12	5	8
−10288·8	−10294·7	5·9	8	1	8	7	1	7
−10241·9	−10243·6	1·7	7	2	6	6	2	3
−10162·7	−10160·1	−2·6	6	3	4	5	3	3
−10084·7	−10085·3	0·6	11	4	7	11	4	8
−9746·1	−9742·6	−3·5	10	3	7	10	3	8
−9707·1	−9709·4	2·3	5	4	2	4	4	1
−9430·3	−9430·3	0·0	9	2	7	9	2	8
−9145·6	−9148·7	3·1	8	1	7	8	1	8
−9014·2	−9021·9	7·7	7	1	7	6	1	6
−8968·8	−8971·2	2·4	6	2	5	5	2	4
−8850·5	−8855·8	5·3	5	3	3	4	3	2
−8716·0	−8717·4	1·4	10	4	6	10	4	7
−8429·4	−8434·4	5·0	4	3	1	3	3	0
−8403·4	−8407·4	4·0	9	3	6	9	3	7
−8125·8	−8127·4	1·6	8	2	6	8	2	7
−7878·2	−7877·8	−0·4	7	1	6	7	1	7
−7755·4	−7765·1	9·7	6	1	6	5	1	5
−7712·5	−7714·0	1·5	5	2	4	4	2	3
−7423·9	−7430·0	6·1	4	3	2	3	3	1
−7362·2	−7363·9	1·7	9	4	5	9	4	6
−7084·0	−7087·5	3·5	8	3	5	8	3	6
−6837·7	−6840·2	2·5	7	2	5	7	2	6
−6519·3	−6524·2	4·9	5	1	5	4	1	4
−6456·8	−6461·6	4·8	4	2	3	3	2	2
−6298·3	−6302·0	3·7	9	6	4	9	4	5
−6279·4	−6283·6	4·2	9	5	4	9	5	5
−6189·0	−6194·9	5·9	3	2	1	2	2	0
−6024·6	−6020·7	−3·9	8	4	4	8	4	5
−5780·9	−5781·2	0·3	7	3	4	7	3	5
−5566·4	−5568·2	1·8	6	2	4	6	2	5
−5381·2	−5383·6	2·4	5	1	4	5	1	5

contd

Table 1 (*continued*).

Observed Frequency/MHz	Calculated Frequency/MHz	Obs.-calc. Frequency/MHz	Identification					
			J''	K''_{-1}	K''_{+1}	J'	K'_{-1}	K'_{+1}
−5294·2	−5299·3	5·1	4	1	4	3	1	3
−5144·6	−5148·1	3·5	3	2	2	2	2	1
−5029·6	−5029·0	−0·6	9	6	3	9	6	4
−4988·0	−4989·4	1·4	8	6	3	8	4	4
−4844·4	−4847·6	3·2	8	5	3	8	5	4
−4725·5	−4725·7	0·2	7	5	3	7	3	4
−4659·2	−4659·8	0·6	7	4	3	7	4	4
−4505·8	−4503·1	−2·7	6	4	3	6	2	4
−4472·0	−4476·5	4·5	6	3	3	6	3	4
−4347·1	−4343·8	−3·3	8	7	2	8	5	3
−4307·5	−4316·0	8·5	5	3	3	5	1	4
−4307·5	−4307·1	−0·4	5	2	3	5	2	4
−4159·3	−4161·2	1·9	4	2	3	4	0	4
−4159·3	−4159·0	−0·3	4	1	3	4	1	4
−4159·3	−4155·0	−4·3	7	7	1	7	5	2
−4087·9	−4087·7	−0·2	3	1	3	2	1	2
−3939·0	−3943·8	4·8	2	1	1	1	1	0
−3903·3	−3905·4	2·1	7	6	2	7	4	3
−3576·4	−3565·7	−10·7	6	5	2	6	3	3
−3437·3	−3441·7	4·4	6	6	1	6	4	2
−3399·6	−3404·5	4·9	10	8	2	10	8	3
−3345·0	−3347·2	2·2	9	7	2	9	7	3
−3299·5	−3305·9	6·4	5	4	2	5	2	3
−3299·5	−3296·4	−3·1	8	6	2	8	6	3
−3238·4	−3243·5	5·1	7	5	2	7	5	3
−3177·3	−3181·7	4·4	6	4	2	6	4	3
−3105·2	−3110·0	4·8	4	3	2	4	1	3
−3105·2	−3107·8	2·6	5	3	2	5	3	3
−3021·4	−3023·6	2·2	4	2	2	4	2	3
−2965·5	−2965·9	0·4	3	2	2	3	0	3
−2924·5	−2927·1	2·6	2	0	2	1	0	1
−2863·4	−2865·4	2·0	5	5	1	5	3	2
−2863·4	−2864·0	0·6	2	1	2	1	1	1
−2418·9	−2421·3	2·4	4	4	1	4	2	2
−2091·9	−2096·9	5·0	3	3	1	3	1	2
−2049·1	−2051·8	2·7	10	9	1	10	9	2
−1894·4	−1896·7	2·3	9	8	1	9	8	2
−1789·7	−1792·3	2·6	8	7	1	8	7	2
−1724·7	−1728·1	3·4	7	6	1	7	6	2
−1687·0	−1692·7	5·7	6	5	1	6	5	2
−1665·6	−1669·6	4·0	2	1	1	2	1	2
−1665·6	−1669·4	3·8	4	3	1	4	3	2
−1665·6	−1668·4	2·8	3	2	1	3	2	2
−1626·6	−1638·6	12·0	10	10	0	10	10	1
−1366·7	−1362·1	−4·6	9	9	0	9	9	1
−1295·8	−1290·7	−5·1	9	9	1	9	9	0
−1124·9	−1123·2	−1·7	8	8	0	8	8	1
−1006·6	−1004·9	−1·7	8	8	1	8	8	0
−924·7	−925·5	0·8	7	7	0	7	7	1
−867·5	−872·3	4·8	9	8	2	9	8	1
−775·2	−772·3	−2·9	6	6	0	6	6	1
−734·9	−735·3	0·4	7	7	1	7	7	0
−662·7	−664·8	2·1	5	5	0	5	5	1
−596·5	−599·5	3·0	4	4	0	4	4	1

contd

Table 1 (*continued*).

Observed Frequency/MHz	Calculated Frequency/MHz	Obs.-calc. Frequency/MHz	Identification					
			J''	K''_{-1}	K''_{+1}	J'	K'_{-1}	K'_{+1}
−556·2	−557·8	1·6	1	1	0	1	1	1
−556·2	−557·7	1·5	2	2	0	2	2	1
−478·2	−478·2	0·0	6	6	1	6	6	0
−432·0	−430·8	−1·2	8	7	2	8	7	1
−233·1	−232·1	−1·0	5	5	1	5	5	0
1·4	−3·4	4·8	7	6	2	7	6	1
1·4	0·0	1·4	4	4	1	4	4	0
210·0	208·7	1·3	3	3	1	3	3	0
384·3	381·0	3·3	2	2	1	2	2	0
399·9	396·7	3·2	6	5	2	6	5	1
505·2	503·9	1·3	1	1	1	1	1	0
549·3	546·5	2·8	9	7	3	9	7	2
761·2	756·9	4·3	5	4	2	5	4	1
1073·1	1067·6	5·5	4	3	2	4	3	1
1073·1	1073·9	−0·8	8	6	3	8	6	2
1320·8	1321·9	−1·1	3	2	2	3	2	1
1517·7	1515·5	2·2	2	1	2	2	1	1
1541·1	1538·4	2·7	7	5	3	7	5	2
1660·7	1663·4	−2·7	0	0	0	1	0	1
1725·6	1727·9	−2·3	2	0	2	2	2	1
1767·2	1763·4	3·8	3	1	2	3	3	1
1838·1	1837·7	0·4	4	2	2	4	4	1
1930·4	1931·0	−0·6	6	4	3	6	4	2
2159·2	2165·9	−6·7	8	5	3	8	7	2
2196·8	2202·0	−5·2	10	7	3	10	9	2
2237·1	2236·1	1·0	7	4	3	7	6	2
2237·1	2246·8	−9·7	5	3	3	5	3	2
2329·5	2340·3	−10·8	6	3	3	6	5	2
2371·1	2373·1	−2·0	10	6	4	10	8	3
2451·0	2460·0	−9·0	5	2	3	5	4	2
2482·8	2486·3	−3·5	4	2	3	4	2	2
2573·9	2580·0	−6·1	4	1	3	4	3	2
2731·1	2738·4	−7·3	8	5	4	8	5	3
2770·7	2778·0	−7·3	1	1	1	2	1	2
2828·6	2838·0	−9·4	1	0	1	2	0	2
2889·0	2897·8	−8·8	8	4	4	8	6	3
3062·6	3069·1	−6·5	7	4	4	7	4	3
3139·9	3143·8	−3·9	7	3	4	7	5	3
3329·8	3336·3	−6·5	6	3	4	6	3	3
3367·6	3366·7	0·9	6	2	4	6	4	3
3551·8	3550·8	1·0	5	2	4	5	2	3
3551·8	3561·0	−9·2	5	1	4	5	3	3
3717·8	3721·0	−3·2	4	1	4	4	1	3
3717·8	3723·6	−5·8	4	0	4	4	2	3
3813·8	3821·6	−7·8	1	1	0	2	1	1
3900·5	3910·2	−9·7	2	0	2	3	0	3
4054·7	4054·7	0·0	8	4	5	8	4	4
4280·6	4281·8	−1·2	11	6	6	11	6	5
4324·7	4325·9	−1·2	7	3	5	7	3	4
4553·8	4558·4	−4·6	6	2	5	6	2	4
4625·1	4653·4	−1·3	10	5	6	10	5	5
4755·2	4754·6	0·6	5	1	5	5	1	4
4901·7	4907·5	−5·8	2	2	1	3	2	2
4984·3	4988·8	−4·5	3	0	3	4	0	4

contd

Table 1 (*continued*).

Observed Frequency/MHz	Calculated Frequency/MHz	Obs.-calc. Frequency/MHz	Identification					
			J''	K''_{-1}	K''_{+1}	J'	K'_{-1}	K'_{+1}
5071·7	5074·9	−3·2	2	1	1	3	1	2
5286·5	5283·1	3·4	8	3	6	8	3	5
5542·4	5544·1	−1·7	7	2	6	7	2	5
5774·6	5770·7	3·9	6	1	6	6	1	5
5913·8	5912·4	1·4	2	2	0	3	2	1
6052·5	6053·9	−1·4	4	0	4	5	0	5
6052·5	6057·3	−4·8	3	2	2	4	2	3
6225·6	6221·5	4·1	9	3	7	9	3	6
6396·6	6396·7	−0·1	12	4	8	12	6	7
6519·2	6513·0	6·2	8	2	7	8	2	6
6788·7	6787·1	1·6	11	3	8	11	5	7
6971·1	6973·8	−2·7	3	3	1	4	3	2
7100·2	7103·2	−3·0	5	0	5	6	0	6
7113·4	7119·9	−6·5	4	1	3	5	1	4
7278·2	7279·4	−1·2	3	2	1	4	2	2
7378·7	7380·6	−1·9	2	1	1	3	3	0
7465·4	7465·5	−0·1	9	2	8	9	2	7
7663·3	7661·6	1·7	12	3	9	12	5	8
7755·6	7754·5	1·2	8	1	8	8	1	7
7927·0	7929·8	−2·8	3	3	0	4	3	1
8050·1	8048·5	1·6	11	2	9	11	4	8
8129·0	8136·6	−7·6	6	1	6	7	1	7
8145·4	8152·3	−6·9	5	1	4	6	1	5
8167·5	8167·4	0·1	4	3	2	5	3	3
8238·7	8241·2	−2·5	4	2	2	5	2	3
8402·6	8402·0	0·6	10	2	9	10	2	8
8722·3	8722·3	0·0	9	1	9	9	1	8
8972·5	8977·4	−4·9	4	4	1	5	4	2
9147·6	9153·9	−6·3	7	1	7	8	1	8
9164·4	9169·7	−5·3	6	1	5	7	1	6
9211·0	9222·5	−11·5	5	2	3	6	2	4
9324·3	9322·3	2·0	11	1	10	11	3	9
9431·4	9433·2	−1·8	4	3	1	5	3	2
9681·6	9674·1	7·5	10	0	10	10	2	9
9700·4	9700·7	−0·3	3	2	1	4	4	0
9864·4	9866·7	−2·3	4	4	0	5	4	1
10152·3	10155·3	−3·0	8	1	8	9	1	9
10171·1	10171·4	−0·3	7	2	6	8	2	7
10218·1	10219·5	−1·4	6	2	4	7	2	5
10390·7	10388·7	2·0	5	3	2	6	3	3
10615·6	10609·9	5·7	11	0	11	11	2	10
10921·0	10919·2	1·8	5	5	1	6	5	2
11143·9	11140·7	3·2	9	1	9	10	1	10
11161·8	11157·0	4·8	8	2	7	9	2	8
11205·2	11204·7	0·5	7	2	5	8	2	6
11282·4	11277·3	5·1	6	4	3	7	4	4
11305·3	11300·3	5·0	6	3	3	7	3	4
11527·8	11520·8	7·0	5	4	1	6	4	2
11727·7	11718·2	9·5	5	5	0	6	5	1
12114·2	12110·1	4·1	10	1	10	11	1	11
12131·4	12126·8	4·6	9	2	8	10	2	9
12177·9	12174·5	3·4	8	3	6	9	3	7
12259·3	12256·4	2·9	7	3	4	8	3	5
12533·6	12523·8	9·8	6	4	2	7	4	3

Table 2. Molecular constants of the 1,4-DMN molecule in the electronic groundstate $S_0(^1A_1)$ and the first electronic excited state $S_1(^1A_1)$ ($\Delta A = A' - A''$ etc.).

$S_0(^1A_1)$		$S_1(^1A_1)$	
A'' MHz	1178·17 (14)	ΔA MHz	−14·420 (64)
B'' MHz	1111·92 (12)	ΔB MHz	−17·046 (67)
C'' MHz	576·54 (10)	ΔC MHz	−7·993 (27)
	$\nu_0(\text{cm}^{-1})$	31491·553 (0·004)	

Indicated errors in the effective rotational constants are the standard deviation of the asymmetric rotor fit. Experimental errors in the effective rotational constants are about four times the indicated errors (see text).

ground state. T_{rot} is the effective rotational temperature of the molecules in the molecular beam, k is the Boltzmann constant and I_0 is the normalized intensity. Since 1,4-DMN is a near oblate symmetric rotor ($\kappa = 0{\cdot}78$) we can approximate $A_{J''K_{-1}''K_{+1}''}$ with the corresponding symmetric top expressions [8]. The spin statistical weight g_n for the electronic ground state is derived in the next section. A fit of the experimental spectrum to equation (1) yielded a rotational temperature of $T_{rot} = 3{\cdot}0 \pm 0{\cdot}3$ K. This value is in agreement with previously determined rotational temperatures for similar molecules under comparable conditions.

4. Internal rotation analysis

It is well known for a single methyl group connected to an asymmetric rotor frame that every rotational state with quantum numbers J, K_{-1}, K_{+1} in the torsional vibration state characterized by the quantum number v gives rise to three torsion-rotation states. These states are indicated by the quantum number σ. There is one non degenerate A state ($\sigma = 0$) and one degenerate E state ($\sigma = \pm 1$). For $K \geqslant 1$ (with K the limiting near oblate or near prolate value), this degenerate E state splits up due to the interaction between the overall rotation and the internal rotation [1]. In 1,4-DMN there are two methyl groups attached to an asymmetric rotor frame. Hence there are nine torsion-rotation states associated with every rotational state in the torsional vibration state characterized by v_1, v_2.

In order to determine the energies of these torsion-rotation states we calculate the different energy terms in the hamiltonian. In this we use the principal axis method (PAM) expressions. The direction of the symmetry axes of the two methyl groups is almost parallel to the b-axis of the molecule (figure 2). In the approximate case that the direction of the symmetry axes of the methyl groups is perpendicular to the a-axis of the molecule, the hamiltonian for the internal rotation in 1,4-DMN can directly be obtained from the internal rotation problem in acetone, and is given to lowest order by [9]:

$$\left.\begin{aligned} H &= H_{rot} + H_{tor} + H_{tt} + H_{rt}, \\ H_{rot} &= AP_a^2 + BP_b^2 + CP_c^2, \\ H_{tor} &= Fp_1^2 + \tfrac{1}{2}V_1(1 - \cos 3\alpha_1) + Fp_2^2 + \tfrac{1}{2}V_2(1 - \cos 3\alpha_2), \\ H_{tt} &= F'(p_1 p_2 + p_2 p_1) + V_{12} \cos 3\alpha_1 \cos 3\alpha_2, \\ H_{rt} &= -2\lambda_c CP_c(p_1 + p_2) - 2\lambda_b BP_b(p_1 - p_2). \end{aligned}\right\} \quad (2)$$

In this equation P_i ($i = a, b, c$) is the total angular momentum operator around the corresponding axis of inertia i and p_i ($i = 1, 2$) is the internal angular momentum operator of methyl group i around its symmetry axis. The angle α_i ($i = 1, 2$) is the internal angle of methyl group i. A, B, and C are the effective rotational constants. These are in this hamiltonian connected to the moments of inertia I by

$$A = \frac{h^2}{8\pi^2}\left(\frac{1}{r_a I_a}\right), \tag{2 a}$$

with

$$r_a = 1 - 2\frac{\lambda_a^2 I_a}{I_a}. \tag{2 b}$$

Similar equations hold for B and C, involving r_b, I_b, and λ_b, r_c, I_c, and λ_c. Here I_α is the moment of inertia of a single methyl group and λ_x is the direction cosine of the symmetry axis of a methyl group to the principal axis of inertia x. By symmetry the direction cosines have the same magnitude for the two methyl groups. The approximation that the symmetry axes of the two methyl groups are perpendicular to the a-axis implies that λ_a is equal to zero. Furthermore we have

$$F = \frac{h^2}{16\pi^2 I_\alpha}\left(\frac{1}{r_b} + \frac{1}{r_c}\right), \tag{2 c}$$

$$F' = \frac{h^2}{16\pi^2 I_\alpha}\left(\frac{1}{r_b} - \frac{1}{r_c}\right). \tag{2 d}$$

The barriers for internal rotation for the methyl groups are given by V_1 and V_2. These are by symmetry equal in 1,4-DMN. The two methyl groups experience a threefold barrier because the naphthalene frame is asymmetric with respect to the position of the two methyl groups. The higher order terms in the barriers are neglected. The coupling between the two methyl groups is given by V_{12}. In our analysis we take $V_{12} = 0$.

The interaction between internal rotation and overall rotation is given by H_{rt}. In 1,4-DMN the two methyl groups are directed almost parallel to the principal b-axis of inertia (figure 2). An estimated value for the direction cosines can be obtained from structure calculations on 1-methylnaphthalene [10]. The values derived in this way are $\lambda_a = 0{\cdot}0026$, $\lambda_b = 1 - 1{\cdot}6 \times 10^{-5}$ and $\lambda_c = 0{\cdot}0051$. This implies that λ_c, the direction cosine of the methyl groups to the unique c-axis in this near oblate symmetric top is almost equal to zero. However, the term $-2\lambda_c CP_c(p_1 + p_2)$ couples states which are nearly degenerate for high J, K_{+1} values and has therefore a first order effect. Despite the fact that λ_c is very small, we will take this term into account. It has been assumed that λ_c has the same sign for both methyl groups. In the analysis this has no further consequences. The term with λ_b interacts between states with different K_{+1} with the selection rules $\Delta J = 0$ and $\Delta K_{+1} = \pm 1$. The contribution of this term is therefore a second order effect. As mentioned before we have made the approximation $\lambda_a = 0$. In this we neglect terms which are also second order effects. The magnitudes of these terms are a factor of λ_a/λ_b less than terms with λ_b and hence negligible. This justifies the approximation $\lambda_a = 0$.

We start the analysis by ignoring the interaction term H_{tt} between the two methyl groups and the interaction term H_{rt} between the internal rotation and the overall rotation. In this case the hamiltonian consists of an asymmetric rotor part H_{rot} and

two uncoupled internal rotors. The wave functions and energies are well known in this case [11].

$$E_{\text{tot}} = E(J, K_{-1}, K_{+1}) + E(v_1, \sigma_1) + E(v_2, \sigma_2), \tag{3}$$

with the corresponding product wave functions $|JK_{-1}K_{+1}\rangle|v_1\sigma_1\rangle|v_2\sigma_2\rangle$. In this formula $E(J, K_{-1}, K_{+1})$ is the normal asymmetric rotor energy and $E(v_i, \sigma_i)$ is the energy of a single internal rotor. The asymmetric rotor wave function are denoted by $|JK_{-1}\ K_{+1}\rangle$ and $|v_i\sigma_i\rangle$ are the single internal rotor wave functions [1].

To determine the electronic spectrum emerging from these energy states, we have to classify these torsion-rotation wave functions according to the symmetry species of the molecular symmetry group. The rigid 1,4-DMN molecule belongs to the C_{2v} molecular point group. In this all carbon atoms are taken in one plane. The torsional tunnelling of the two methyl groups contains nine feasible operations. Hence the molecular symmetry group of 1, 4-DMN with torsional tunnelling contains 36 elements, G_{36} [12]. This is, e.g., the molecular symmetry group for acetone with torsional tunnelling. With the ground state barrier of 770 cm^{-1} [5], only the ground torsional vibration state is populated in our molecular beam, and we set $v_1 = v_2 = 0$. The wave functions are classified according to the symmetry species of G_{36}, and the nuclear spin statistical weight is calculated. There are 12 hydrogen atoms in the

Table 3. Symmetry species and statistical weights of the basis wave functions in G_{36}.

K_{-1}	K_{+1}	σ_1	σ_2	Symmetry	Statistical weight
e	*e*	0	0	A_1	528
		0	±1	G	1024
		±1	0		
		+1	−1	E_1	256
		−1	+1		
		+1	+1	E_3	272
		−1	−1		
e	*o*	0	0	A_3	528
		0	±1	G	1024
		±1	0		
		+1	−1	E_2	256
		−1	+1		
		+1	+1	E_3	272
		−1	−1		
o	*e*	0	0	A_4	496
		0	±1	G	1024
		±1	0		
		+1	−1	E_2	256
		−1	+1		
		+1	+1	E_4	240
		−1	−1		
o	*o*	0	0	A_2	496
		0	±1	G	1024
		±1	0		
		+1	−1	E_1	256
		−1	+1		
		+1	+1	E_4	240
		−1	−1		

molecule. They give rise to 4096 nuclear spin functions, divided among the symmetry species as

$$^{n}\Gamma = 528A_1 + 496A_4 + 136E_1 + 120E_2 + 136E_3 + 120E_4 + 512G.$$

In table 3 the wave functions are given together with the statistical weights. Every rotational state J, K_{-1}, K_{+1} gives rise to nine rotation-torsion states characterized by the quantum numbers J, K_{-1}, K_{+1}, σ_1, σ_2 ($\sigma_i = 0, \pm 1$). The non degenerate A_i ($i = 1 \ldots 4$) states have both $\sigma_1 = \sigma_2 = 0$. The fourfold degenerate G states have either σ_1 or σ_2 equal to zero, while the two twofold degenerate E_i ($i = 1 \ldots 4$) states have both σ_1 and σ_2 unequal to zero.

With equation (3) we see that the two E_i states are also degenerate for each rotational state as long as the interaction terms H_{rt} and H_{tt} in the hamiltonian are neglected. The energy splitting between the A_i and G states equals the energy splitting between the G and the two E_i states. The magnitude is equal to the energy splitting for one internal rotor between the A ($\sigma = 0$) and E ($\sigma = \pm 1$) states. This is exactly as expected from the simple addition of the energy levels of two independent rotors. An energy scheme is depicted in figure 4.

The rotation of the methyl groups does not affect the electronic transition dipole moment and the selection rule $\Delta\sigma_1 = \Delta\sigma_2 = 0$ holds for an electronic transition. In the corresponding electronic spectrum we thus expect three lines for each rotational

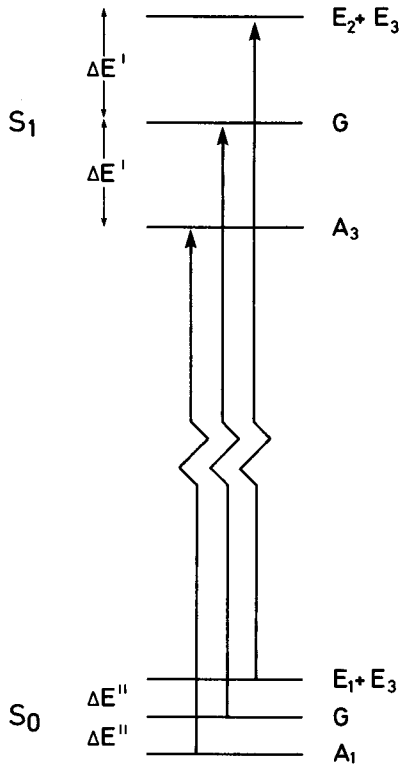

Figure 4. Energy level scheme in 1,4-DMN for a transition $(K'_{-1}, K'_{+1}) = (e, o) \leftarrow (K''_{-1}, K''_{+1}) = (e, e)$ The splittings of the lines in the spectrum amount to $\Delta E' - \Delta E''$.

transition. This is indicated in figure 4. The splitting of the lines in the spectrum $\Delta E = \Delta E' - \Delta E''$ is thus determined by the difference in splittings in the upper and lower electronic states. The intensities of these three lines are given by the nuclear spin statistical weight and are

$$A_1 : G : E_1,\ E_3 = A_3 : G : E_2,\ E_3 = 528 : 1024 : 528$$

$$\text{for} \quad (K_{-1}, K_{+1}) = (e, e) \quad \text{or} \quad (e, o),$$

$$A_2 : G : E_1,\ E_4 = A_4 : G : E_2,\ E_4 = 496 : 1024 : 496$$

$$\text{for} \quad (K_{-1}, K_{+1}) = (o, e) \quad \text{or} \quad (o, o).$$

Here the degeneracy of the E states is taken into account.

From the splitting of 40 ± 1 MHz between the three lines in the spectrum we can calculate the barrier height V_1 to internal rotation. This results in a barrier height of $570\,\text{cm}^{-1}$ in the excited electronic state S_1. In this we have taken a barrier height to internal rotation of $770\,\text{cm}^{-1}$ [5] in the electronic ground state S_0. However, the splitting of the lines in the electronic spectrum is dominated by the splitting $\Delta E'$ in the excited electronic state: a 10 per cent error in the ground state barrier height results in only a 1 per cent error in the excited state barrier height. The uncertainty of 1 MHz in the measured splitting gives an 0·5 percent uncertainty in the calculated barrier height. We conclude therefore that the barrier height to internal rotation for the methyl groups in the excited S_1 electronic state is $570 \pm 10\,\text{cm}^{-1}$.

With these results the contributions of the various neglected interaction terms in the hamiltonian to the energy can be estimated. Useful basis wave functions for the calculations of the matrix elements are the Wang functions [13] $|S_{JKM\gamma}\rangle$ for the asymmetric rotor part and the product of the single internal rotor wave functions $|v_1\sigma_1\rangle|v_2\sigma_2\rangle$ for the internal rotor part. As mentioned before we take $v_1 = v_2 = 0$. Due to the large energy difference between states with different torsional quantum number v we neglect all matrix elements off diagonal in v. Only states with the same symmetry interact. Therefore we calculate the energy contributions from the interaction terms in the hamiltonian for each symmetry species separately.

A state with A_i $(i = 1 \ldots 4)$ symmetry has both $\sigma_1 = \sigma_2 = 0$ (table 3). For a single internal rotor the matrix elements are well known [12]:

$$\langle v = 0, \sigma = 0 | p | v = 0, \sigma = 0\rangle = 0,$$

$$\langle v = 0, \sigma = 1 | p | v = 0, \sigma = 1\rangle = w_{01}^1.$$

The matrix elements w_{01}^1 are given for the different barrier heights [12]. With these matrix elements it is clear from equation (2) that the interaction terms H_{tt} and H_{rt} do not contribute to the energy of a state with $\sigma_1 = \sigma_2 = 0$. Therefore it is possible to fit the A_i states to an asymmetric rotor hamiltonian. This yields the effective rotational constants in the electronic ground state and the first excited electronic state. In the present asymmetric rotor fit we have used the central line of each group of three, i.e. transitions connecting states with G symmetry. However, the constant splitting in the spectrum between the lines connecting states with G symmetry and the lines connecting states with A_i symmetry guarantees the correctness of our fit.

A state with G symmetry has either $\sigma_1 = 0$ or $\sigma_2 = 0$. Therefore the contribution of H_{tt} equals zero. The interaction term H_{rt} has non zero matrix elements. The contribution of this term to the energy consists of two parts, $-2\lambda_c CP_c(p_1 + p_2)$ and $-2\lambda_b BP_b(p_1 - p_2)$. It is clear that only states with the same σ_1 and σ_2 interact.

The first term, $-2\lambda_c\, CP_c(p_1 + p_2)$ interacts between the symmetric and antisymmetric Wang functions with the same J and K_{+1}. These two states of G symmetry are for high J and K_{+1} values nearly degenerate. The effect of the hamiltonian interaction term on the energy states is an additional contribution to the K_{+1} splitting besides the asymmetry splitting. For nearly degenerate rotational states J, K_{+1}, this interaction term results in a splitting with magnitude $2\lambda_c\, CK_{+1}w^1_{01}$. This amounts to $0{\cdot}002\, K_{+1}$ MHz. Here a barrier to internal rotation of $V_1 = 570\,\mathrm{cm}^{-1}$ is taken as deduced for the electronic excited state. In the ground electronic state the splitting will be even less.

It is clear that with the present resolution the K_{+1} splitting due to the interaction of the internal rotation and overall rotation is undetectable in the spectrum of the electronic transition in 1,4-DMN. This is caused by the fact that the symmetry axes of the two methyl groups are nearly perpendicular to the principal c-axis of inertia in this near oblate symmetric top. In similar molecules with comparable barrier heights this splitting can show up in a high resolution laser induced fluorescence spectrum as demonstrated for 1-methylnaphthalene [14]. The appearance of the splitting linear in the rotational quantum number K (i.e. K_{+1} for a near oblate symmetric top and K_{-1} for a near prolate symmetric top) for lines not split by the asymmetric rotor splitting gives for a perpendicular band in general the possibility to determine the barrier heights in both electronic states independently. The difference in K splitting between the transitions $K' = K'' + 1 \leftarrow K''$ and $K' = K'' - 1 \leftarrow K''$ gives directly the barrier to internal rotation in the excited electronic state. In the same way the difference in K-splitting between the transitions $K' \leftarrow K'' = K' + 1$ and $K' \leftarrow K'' = K' - 1$ gives the barrier height in the ground electronic state.

The second interaction term, $-2\lambda_b\, BP_b(p_1 - p_2)$ couples K_{+1} states with states with $K_{+1} \pm 1$. The energy difference between these states is large compared to the matrix elements. Therefore the contribution to the energy can be calculated by second order perturbation theory. The energy shift for a rotational state characterized by the quantum numbers J and K_{+1} is for $K_{+1} \geqslant 2$ given by

$$\Delta E(J, K_{+1}) = \frac{(w^1_{01}\lambda_b B)^2}{A - B}\left[\frac{J(J+1) - K_{+1}(K_{+1}+1)}{2K_{+1}+1} - \frac{J(J+1) - K_{+1}(K_{+1}-1)}{2K_{+1}-1}\right].$$

Here for simplicity the symmetric rotor energy differences are used. The factor in front is equal to 2×10^{-4} MHz for a barrier height of $570\,\mathrm{cm}^{-1}$. We again conclude that the effect of this interaction term is too small to show up in the electronic spectrum of 1,4-DMN with the present resolution.

A state with E_i symmetry has in general contributions of both the interaction terms H_{tt} and H_{rt}. The magnitude of the contribution of H_{tt} is $\frac{1}{2}F'(w^1_{01})^2$. This term is about 7×10^{-5} MHz in 1,4-DMN with the previous assumptions. The sign of this term is the same for states with E_1 and E_2 symmetry and opposite for states with E_3 and E_4 symmetry. It is clear from table 3 that this term in the hamiltonian splits the two nearly degenerate E_i states and corresponds to the energy difference between geared and anti-geared rotation. The contribution of the term $-2\lambda_c CP_c(p_1 + p_2)$ of H_{rt} equals zero. This is because states with the same E_i symmetry have different J or K_{+1} quantum numbers as seen in table 3. The contribution of the second term $-2\lambda_b BP_b(p_1 - p_2)H_{rt}$ equals zero too. For states with $\sigma_1 = \sigma_2$ the contribution of each rotor is equal in magnitude but with opposite signs, while states with $\sigma_1 = -\sigma_2$ do not interact due to the different symmetry of the Wang functions.

5. Summary and conclusion

It has been shown that the $S_1(^1A_1) \leftarrow S_0(^1A_1)$ electronic spectrum of 1,4-DMN can be explained by the simple model of two independent internal rotors attached to an asymmetric rotor frame. The corresponding torsion-rotation wave functions are classified according to the molecular symmetry group G_{36}. There are nine torsion-rotation states connected to every rotational state: a nondegenerate A_i state, a fourfold degenerate G state and two twofold degenerate E_i states. We have fitted the states with G symmetry to an asymmetric rotor hamiltonian. This results in the effective rotational constants for the upper and lower electronic states listed in table 2. Although there is no experimental structure known for 1,4-DMN, a neutron diffraction study on 1,5-DMN [15] allows us to derive a configuration for the 1,4-DMN molecule. The rotational constants calculated from this estimated structure differ by only 0·3 per cent with the rotational constants derived from the present results. In this the effective rotational constants are corrected for the internal rotation effect (equation (2 *a*)). These results are well within the 1 per cent error in the calculated rotational constants, derived from the estimated structure.

The absence of the K_{+1} splitting due to the interaction of overall and internal rotation in our high resolution spectrum makes it impossible to determine both barrier heights seperately. However, the results from spin relaxation measurements [5] gives a barrier height of about 770 cm^{-1} in the electronic ground state. With this result and the measured splitting of 40 MHz in the high resolution spectrum the barrier to internal rotation in the electronic excited S_1 state is calculated to be 570 cm^{-1}, with an error of about 10 cm^{-1}.

We would like to thank Professor J. Reuss for his stimulating interest. This work is part of the research program of the Stichting voor Fundamenteel Onderzoek der Materie (FOM) and has been been made possible by financial support from the Nederlandse Organisatie voor Zuiver Wetenschappelijk Onderzoek (ZWO).

References

[1] Gordy, W., and Cook, R. L., 1970, *Microwave Molecular Spectra* (Interscience).
[2] Meerts, W. L., and Ozier, I., 1978, *Phys. Rev. Lett.*, **41**, 1109.
[3] See, for example, Okuyama, K., Hasegawa, T., Ito, M., and Mikami, N., 1984, *J. phys. Chem.*, **88**, 1711.
[4] Ebben, M., Spooren, R., ter Meulen, J. J., and Meerts, W. L., 1989, *J. phys.* D, **22**, 1549.
[5] Ladner, K. H., Dalling, D. K., and Grant, D. M., 1976, *J. phys. Chem.*, **80**, 1783.
[6] Majewski, W. A., and Meerts, W. L., 1984, *J. molec. Spectrosc.*, **104**, 271.
[7] Gerstenkorn, S., and Luc, P., 1978, *Atlas du Spectroscopie d'Absorption de la Molecule d'Iode* (Centre National de la Recherche Scientifique). Gerstenkorn, S., and Luc, P., 1979, *Rev. phys. appl.*, **14**, 791.
[8] Herzberg, G., 1966, *Molecular Spectra and Molecular Structure*, Vol. 2 (Van Nostrand Company Inc.).
[9] Swalen, J. D., and Costain, C. C., 1959, *J. chem. Phys.*, **31**, 1562.
[10] George, P., Bock, C. W., Stezowski, J. J., Hildenbrand, T., and Glusker, J. P., 1988, *J. phys. Chem.*, **92**, 5656.
[11] Lin, C. C., and Swalen, J. D., 1959, *Rev. mod. Phys.*, **31**, 841.
[12] Bunker, P., 1979, *Molecular Symmetry and Spectroscopy* (Academic Press).
[13] Wang, S. C., 1929, *Phys. Rev.*, **34**, 243.
[14] Tan, X. Q., Majewski, W. A., Meerts, W. L., Plusquelic, D. F., and Pratt, D. W., 1989 *J. chem. Phys.*, **90**, 2521.
[15] Ferraris, G., Jones, D. W., Yerkess, J., and Bartle, K. D., 1972, *J. chem. Soc. Perkin II*, p. 1628.